The Chemistry of CO$_2$ Capture in an Amine-Functionalized Metal–Organic Framework under Dry and Humid Conditions

Robinson W. Flaig,[†] Thomas M. Osborn Popp,[†,⊥] Alejandro M. Fracaroli,[†,‡] Eugene A. Kapustin,[†] Markus J. Kalmutzki,[†] Rashid M. Altamimi,[§] Farhad Fathieh,[†] Jeffrey A. Reimer,[⊥,#] and Omar M. Yaghi*,[†,§]

[†]Department of Chemistry, University of California–Berkeley; Materials Sciences Division, Lawrence Berkeley National Laboratory; Kavli Energy NanoSciences Institute at Berkeley; and Berkeley Global Science Institute, Berkeley, California 94720, United States
[⊥]Department of Chemical and Biomolecular Engineering, University of California–Berkeley, Berkeley, California 94720, United States
[‡]Instituto de Investigaciones en Fisicoquímica de Córdoba, INFIQC–CONICET, Facultad de Ciencias Químicas, Departamento de Química Orgánica, Universidad Nacional de Córdoba, Ciudad Universitaria, X5000HUA Córdoba, Argentina
[§]King Abdulaziz City for Science and Technology (KACST), Riyadh 11442, Saudi Arabia
[#]Materials Sciences Division, Lawrence Berkeley National Laboratory, Berkeley, California 94720, United States

S *Supporting Information*

ABSTRACT: The use of two primary alkylamine functionalities covalently tethered to the linkers of IRMOF-74-III results in a material that can uptake CO$_2$ at low pressures through a chemisorption mechanism. In contrast to other primary amine-functionalized solid adsorbents that uptake CO$_2$ primarily as ammonium carbamates, we observe using solid state NMR that the major chemisorption product for this material is carbamic acid. The equilibrium of reaction products also shifts to ammonium carbamate when water vapor is present; a new finding that has impact on control of the chemistry of CO$_2$ capture in MOF materials and one that highlights the importance of geometric constraints and the mediating role of water within the pores of MOFs.

Metal–organic frameworks (MOFs) are emerging as effective materials for selective CO$_2$ chemisorption with high uptake due to the ease with which they may be tuned by the pre- and post-synthetic modification of their building units.[1−3] To date, the most successful MOFs for CO$_2$ capture have included alkylamine-functionalized (R$_1$NHR$_2$, or RNH$_2$) pores. These alkylamines have been shown to selectively react with CO$_2$, forming covalent C−N bonds, yielding great low-pressure (<100 Torr) uptake and selectivity, yet only ammonium carbamate is reported as the product of CO$_2$ capture.[4−10] Previously, we demonstrated that the pores of IRMOF-74-III {Mg$_2$(3,3″-dioxido-[1,1′:4′,1″-terphenyl]-4,4″-dicarboxylate)} can be designed and functionalized with one primary alkylamine covalently attached to each linker leading to enhanced CO$_2$ capture.[6] Here, we report on a new, diamine-functionalized MOF system, IRMOF-74-III-(CH$_2$NH$_2$)$_2$ {Mg$_2$(2′,5′-bis(aminomethyl)-3,3″-dioxido-[1,1′:4′,1″-terphenyl]-4,4″-dicarboxylate)}, and demonstrate its framework chemistry with CO$_2$ under dry and humid conditions. This study contributes to the fundamental understanding of CO$_2$ capture in MOFs under conditions relevant to those required in

practice. Although examples of carbamic acid formation in organic molecular crystals, surface modified silica, and porous silica are reported, control of the CO$_2$-binding chemistry has not been demonstrated.[11−15] We show that the equilibrium of chemisorbed CO$_2$ shifts at the time when CO$_2$ is introduced to the system from primarily carbamic acid to ammonium carbamate depending upon the absence or presence of water, respectively. Accordingly, understanding this chemistry is crucial to achieving control over which of the two chemisorption products is formed, as each species' unique properties may make it desirable for specific carbon capture applications.[14,15]

The synthesis and characterization of organic linkers and extended structure, IRMOF-74-III-(CH$_2$NH$_2$)$_2$, was carried out according to previously reported conditions [see Supporting Information (SI), Sections S2 and S3].[6] Because the presence of free amines on the organic struts disrupts the synthesis of the extended structure, the two primary amine functional groups were incorporated into IRMOF-74-III as Boc-protected (−Boc = *tert*-butyloxycarbonyl) derivatives.[16] The quantitative removal of the −Boc protecting groups from the framework structure by microwave irradiation (SI, Section S4) was confirmed by solid state cross-polarization magic angle spinning nuclear magnetic resonance spectroscopy (CP-MAS NMR), and Fourier transform infrared spectroscopy (FT-IR), as well as solution phase NMR of the acid-digested material (SI, Sections S5, S6, and S7). Powder X-ray diffraction (PXRD) and nitrogen adsorption isotherm experiments confirmed that the framework maintained its structural integrity and porosity after post-synthetic deprotection of the −Boc groups (SI, Sections S8 and S9).

To confirm that CO$_2$ binds in a chemisorptive fashion and that it can be removed afterwards, CO$_2$ isotherms for IRMOF-74-III-(CH$_2$NH$_2$)$_2$ were measured at 25 °C (Figure 1). This compound shows similar capacity (67 cm^3 g$^{−1}$) to the
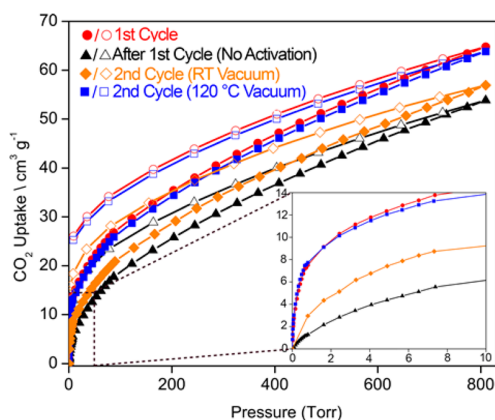
Figure 1. CO_2 isotherms (closed symbols = adsorption; open symbols = desorption) for IRMOF-74-III-$(CH_2NH_2)_2$. In red, after synthesis and activation; in black, after first carbon dioxide isotherm (no activation); in orange, after room temperature activation 12 h; in blue, after 120 °C heating 2 h. (Inset) Expansion of the low pressure range.

previously reported IRMOF-74-III-CH_2NH_2 (75 cm^3 g^{-1}) at 800 Torr, indicating similar physisorption behavior of the materials. In the low pressure range (<100 Torr), however, the IRMOF-74-III-$(CH_2NH_2)_2$ compound significantly out-performs its monoamine counterpart, collecting 2.33 times the amount of CO_2 per gram of material at identical pressures (SI, Section S10), indicative of enhanced chemisorption. The behavior of the material after different activation conditions was also studied (Figure 1). After the first CO_2 isotherm measurement, three separate experiments were conducted: first, a subsequent isotherm was measured without any activation of the material. Investigation of this isotherm reveals a *ca.* 17%

drop in CO_2 uptake at 800 Torr, and a *ca.* 83% drop in CO_2 uptake at 0.8 Torr, compared to the as-synthesized, activated material. This suggests that the amine moieties capture the CO_2 by covalent bond formation. The next isotherm was measured after activating the material under dynamic vacuum at 25 °C for 12 h. Investigation of this isotherm reveals a 12% drop in CO_2 uptake at 800 Torr, and a 61% drop in CO_2 uptake at 0.8 Torr. This indicates that only a portion of the amine-CO_2 bonds are broken simply by applying vacuum as shown in Figure 2. Finally, an isotherm was measured after activating the material under vacuum for 2 h at 120 °C. This isotherm showed no drop in CO_2 uptake in both the high and low pressure regions, indicating full regeneration of the material.

The nature of the covalent bond being formed upon CO_2 chemisorption was examined by solid state ^{13}C and ^{15}N CP-MAS NMR of 50% ^{15}N-enriched IRMOF-74-III-$(CH_2NH_2)_2$ (Figure 2). The ^{13}C spectrum (Figure 2a) shows the carbonyl phenoxide peaks at 173 and 166 ppm respectively, as well as the aromatic peaks between 110 and 150 ppm. Of particular note is the CH_2 resonance with two features at 48.6 and 44.0 ppm. Though only one resonance here is expected, this pair of peaks was consistently observed with similar intensity ratios across several tested samples. Likewise, a pair of amine peaks is observed in the ^{15}N spectrum at 30.3 and 25.4 ppm (Figure 2d), where only one amine resonance is expected. These two peaks are surmised to emanate from two distinct conformations of the linkers based on the torsional angle of the central phenyl ring, yielding two distinct amine positions with slightly different chemical shifts. To characterize the chemisorption products of CO_2, samples were exposed to 675 Torr of $^{13}CO_2$ (99% ^{13}C atom basis) in a sealed dosing apparatus for 24 h. (SI, Section S5). The appearance of a highly intense peak in the ^{13}C spectrum (Figure 2b, in red) with a maximum at 160.3 ppm
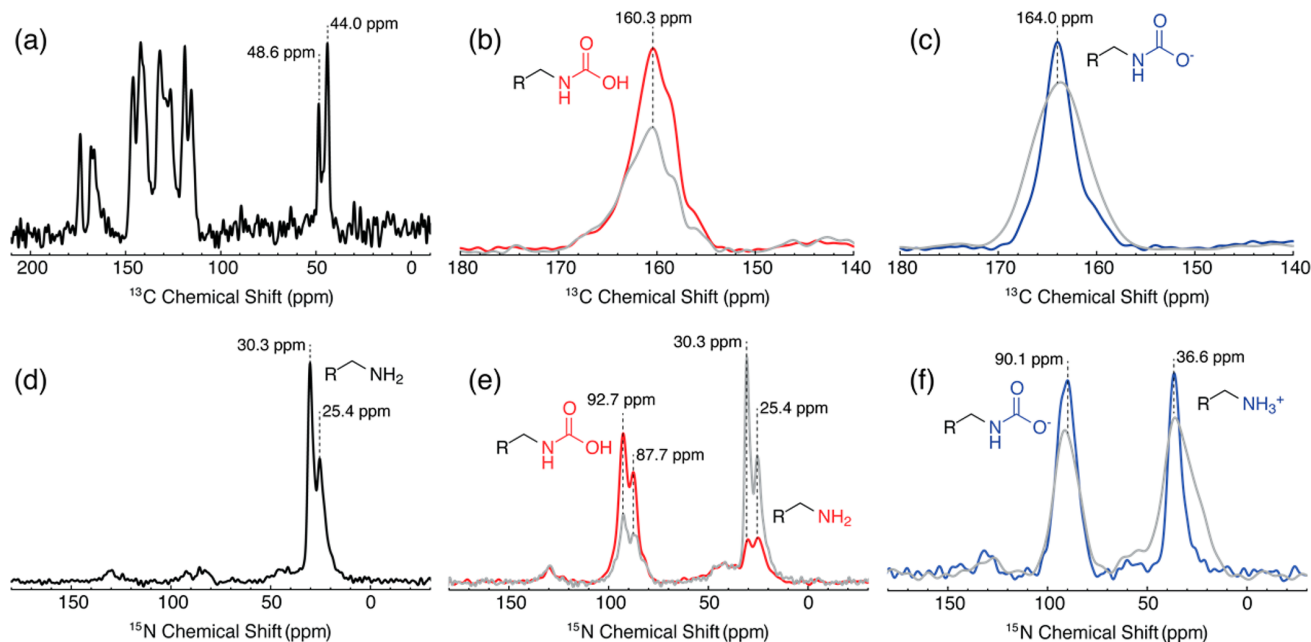

Figure 2. (a) ^{13}C CP-MAS NMR for IRMOF-74-III-$(CH_2NH_2)_2$. (b) ^{13}C CP-MAS NMR after exposure to 675 Torr $^{13}CO_2$ for 24 h (red) and after vacuum for 24 h (gray). (c) ^{13}C CP-MAS NMR after exposure to 95% relative humidity (RH) N_2 atmosphere for 24 h followed by 675 Torr $^{13}CO_2$ for 24 h (blue), and after vacuum for 24 h (gray). (d) ^{15}N CP-MAS NMR for 50% ^{15}N-enriched IRMOF-74-III-$(CH_2NH_2)_2$. (e) ^{15}N CP-MAS NMR after exposure to 675 Torr $^{13}CO_2$ for 24 h (red) and after vacuum for 24 h (gray). (f) ^{15}N CP-MAS NMR after exposure to N_2 atmosphere at 95% RH for 24 h followed by 675 Torr $^{13}CO_2$ for 24 h (blue) and after vacuum for 24 h (gray).

and right-shoulder features at *ca.* 158 and 156 ppm confirmed that the $^{13}CO_2$ was adsorbed by reaction with the primary amines to form a new species. In contrast to our previous study in which a broad peak spanning 164−160 ppm was assigned to a mixture of carbamate and carbamic acid, this sharp, narrow peak is assigned as primarily carbamic acid. This assertion is consistent with chemical shifts observed and/or calculated for carbamic acid in various structural configurations in other solid CO_2 sorbents.[6,12,14,17] The full width at half-maximum line width of 350 Hz and asymmetric shape of this resonance suggest an inhomogeneous broadening arising from multiple overlapping carbamic acid sites, with each site likely varying slightly in its configuration and hydrogen bonding environment.

Further support of the assignment of this resonance as carbamic acid was gathered via ^{15}N CP-MAS NMR (Figure 2 in red, SI, Section S5). The presence of two residual amine peaks at 30.3 and 25.4 ppm was observed, indicating that complete saturation of the alkylamine moieties was not achieved upon exposure to $^{13}CO_2$ at 675 Torr. Two peaks at 92.7 and 87.7 ppm appear at the expense of the amine peaks, suggesting that this difference in chemical shift, arising from conformations of the linkers, carries over to the chemisorbed products as well. Critically, as no major peak is observed that can be assigned as ammonium, we assign these two downfield peaks as carbamic acid ^{15}N sites. However, when the MOF was exposed to 95% relative humidity (RH) conditions prior to loading with $^{13}CO_2$, a significant new peak at 36.6 ppm is observed along with a peak at 90.1 ppm (Figure 2f, blue). Though these CP-MAS spectra are not quantitative with respect to integration, their similar magnitudes suggest that the species observed here is ammonium carbamate, with the peak at 36.6 ppm being ammonium. The assignment of the adsorbed species as ammonium carbamate is supported by the change in the ^{13}C chemical shift maximum for the 95% RH-treated material to 164.0 ppm (Figure 2c, blue), consistent with previous reports of the ^{13}C chemical shift of carbamate.[12,14,17,18] Though some small portion of this ^{13}C signal may be attributable to bicarbonate, as has been discussed in studies of amine-tethered porous silicas,[18] the ^{15}N spectrum enables us to assert that the dominant amine-CO_2 chemisorption product in humid conditions is ammonium carbamate. The peak splitting observed in the dry adsorption spectrum is lost upon exposure to 95% RH, suggesting that the inter-linker interaction required to produce the ion pair ammonium carbamate alters the torsional angle of the central phenyl ring on the linkers to result in one major structural conformation. This shift to ammonium carbamate from carbamic acid occurs as a function of the amount of water vapor present, with MOF samples exposed to atmospheric moisture (50% RH) exhibiting signal contributions from both carbamic acid and carbamate (SI, Section S5).

Although the role of water is critical to this chemistry, initial examination in modeled IRMOF-74-III-$(CH_2NH_2)_2$ of the separation between primary amines points to geometric constraints within the pores as also being operative. To further understand the amine−amine distances and their contribution to this unique chemistry, we modeled the conformation of the linkers (Figure 3, SI Section S11) in IRMOF-74-III-$(CH_2NH_2)_2$. Because the amines are introduced to the material as their −Boc protected counterparts, steric hindrance plays a significant role in their final orientation. When considering amine geometries that would facilitate formation of carbamic acids, two possible intermethylene distances (staggered amine
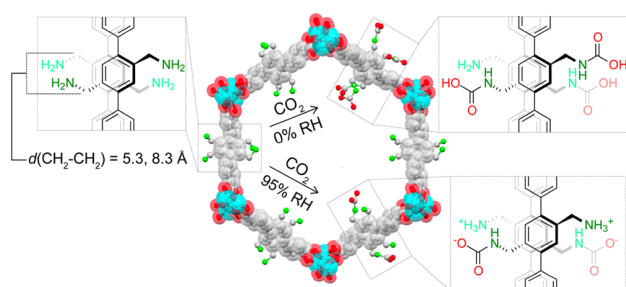
Figure 3. View of modeled IRMOF-74-III-$(CH_2NH_2)_2$ [staggered amine] structure down the crystallographic *c*-axis, depicting the three possible pore environments before (left pore wall) and after exposure to CO_2 under 95% RH (bottom right pore wall) and dry (upper right pore wall) conditions. Dashed boxes clarify the chemisorbed species upon reaction between linker-based alkylamine and CO_2 under the respective conditions. H atoms are omitted for clarity. Color code: C, gray; O, red; N, green; and Mg, blue.

conformation), 5.3 and 8.3 Å, were of particular interest since similar intermethylene distances have been found in molecular carbamic acids (5.982(4) Å, and 8.017(1) Å).[11,15] The similarities between these distances and those in IRMOF-74-III-$(CH_2NH_2)_2$ support the notion of carbamic acid formation in the absence of a proton-transfer species (in the present case, water) which would generate ammonium carbamate.

For additional experimental support of these two species, FT-IR (SI, Section S6), combined thermogravimetric analysis, differential scanning calorimetry, mass spectrometry (TGA-DSC-MS, SI Section S12), and breakthrough measurements (SI, Section S13) were performed. Samples of IRMOF-74-III-$(CH_2NH_2)_2$ exposed to CO_2 were also analyzed using TGA-DSC-MS. The sample lost 12 mass % of CO_2 ($m/z = 44$) at relatively low temperature (onset at 47 °C) after exposure to dry CO_2. Humidified (95% RH) samples of IRMOF-74-III-$(CH_2NH_2)_2$ that were exposed to CO_2 exhibit a mass loss of 10 mass % corresponding to CO_2 ($m/z = 44$) and H_2O ($m/z = 18$) at higher temperature (onset at 65 °C). The results of the thermal analysis indicate CO_2 is more strongly bound as ammonium carbamate as opposed to carbamic acid under wet and dry conditions, respectively. Additionally, the decrease in mass loss under humid conditions supports the conclusion of two amines participating in ammonium carbamate formation versus one amine forming carbamic acid upon reaction with CO_2. The dynamic adsorption capacity, as measured by breakthrough time, remained the same under dry (900 ± 10 s g^{-1}, 1.2 mmol g^{-1}) and 65% RH (890 ± 10 s g^{-1}, 1.2 mmol g^{-1}) conditions (SI, Section S13). This appears counterintuitive given the TGA-DSC-MS results, but is justified by the fact that at 50% RH (SI, Section S5) we observe a mixture of carbamate and carbamic acid in the solid state NMR. This mixture would likely be the result of initial carbamic acid generation, with subsequent proton transfer to form ammonium carbamates, and thus the kinetics of CO_2 capture would be dictated by the formation of the former species.

To investigate the difference in thermal properties between ammonium carbamate and carbamic acid in IRMOF-74-III-$(CH_2NH_2)_2$ and their impact on regeneration of the material, vacuum was applied for 24 h at room temperature to the NMR samples previously exposed to $^{13}CO_2$, and solid state CP-MAS NMR was performed. Under dry loading conditions, the ^{13}C carbamic acid resonance at 160.3 ppm is significantly reduced after vacuum (Figure 2b, gray), and the ^{15}N carbamic acid

resonances at 92.7 and 87.7 ppm decrease as the two amine peaks at 30.3 and 25.4 ppm rise in intensity (Figure 2e, gray). For the sample exposed to both 95% RH and $^{13}CO_2$, room temperature vacuum activation appears much less effective (Figure 2c,f), with only minor loss of signal observed for the carbamate resonance in both the ^{13}C and ^{15}N spectra. This is consistent with the TGA-DSC-MS results, where the onset point of CO_2 desorption as carbamate occurs 18 °C higher than for carbamic acid.

■ ASSOCIATED CONTENT

Ⓢ Supporting Information

The Supporting Information is available free of charge on the ACS Publications website at DOI: 10.1021/jacs.7b06382.

Methods and additional data (PDF)

■ AUTHOR INFORMATION

Corresponding Author
*yaghi@berkeley.edu

ORCID Ⓘ
Robinson W. Flaig: 0000-0003-3090-4724
Alejandro M. Fracaroli: 0000-0003-3016-6813
Eugene A. Kapustin: 0000-0003-4095-9729
Omar M. Yaghi: 0000-0002-5611-3325

Notes
The authors declare no competing financial interest.

■ ACKNOWLEDGMENTS

■ REFERENCES

(1) Cohen, S. M. *Chem. Rev.* **2012**, *112*, 970.
(2) Belmabkhout, Y.; Guillerm, V.; Eddaoudi, M. *Chem. Eng. J.* **2016**, *296*, 386.
(3) Schoedel, A.; Ji, Z.; Yaghi, O. M. *Nat. Energy* **2016**, *1*, 16034.
(4) McDonald, T. M.; D'Alessandro, D. M.; Krishna, R.; Long, J. R. *Chem. Sci.* **2011**, *2*, 2022.
(5) Planas, N.; Dzubak, A. L.; Poloni, R.; Lin, L.-C.; McManus, A.; McDonald, T. M.; Neaton, J. B.; Long, J. R.; Smit, B.; Gagliardi, L. *J. Am. Chem. Soc.* **2013**, *135*, 7402.
(6) Fracaroli, A. M.; Furukawa, H.; Suzuki, M.; Dodd, M.; Okajima, S.; Gándara, F.; Reimer, J. A.; Yaghi, O. M. *J. Am. Chem. Soc.* **2014**, *136*, 8863.
(7) Li, L.-J.; Liao, P.-Q.; He, C.-T.; Wei, Y.-S.; Zhou, H.-L.; Lin, J.-M.; Li, X.-Y.; Zhang, J.-P. *J. Mater. Chem. A* **2015**, *3*, 21849.
(8) McDonald, T. M.; Mason, J. A.; Kong, X.; Bloch, E. D.; Gygi, D.; Dani, A.; Crocellà, V.; Giordanino, F.; Odoh, S. O.; Drisdell, W. S.; Vlaisavljevich, B.; Dzubak, A. L.; Poloni, R.; Schnell, S. K.; Planas, N.; Lee, K.; Pascal, T.; Wan, L. F.; Prendergast, D.; Neaton, J. B.; Smit, B.; Kortright, J. B.; Gagliardi, L.; Bordiga, S.; Reimer, J. A.; Long, J. R. *Nature* **2015**, *519*, 303.
(9) Liao, P.; Chen, X.; Liu, S.; Li, X.; Xu, Y.; Tang, M.; Rui, Z.; Ji, H.; Zhang, J.; Chen, X. *Chem. Sci.* **2016**, *7*, 6528.
(10) Gómora-Figueroa, A. P.; Mason, J. A.; Gonzalez, M. I.; Bloch, E. D.; Meihaus, K. R. *Inorg. Chem.* **2017**, *56*, 4308.
(11) Aresta, M.; Ballivet-Tkatchenko, D.; Dell'Amico, D. B.; Boschi, D.; Calderazzo, F.; Labella, L.; Bonnet, M. C.; Faure, R.; Marchetti, F. *Chem. Commun.* **2000**, *8*, 1099.
(12) Pinto, M. L.; Mafra, L.; Guil, J. M.; Pires, J.; Rocha. *Chem. Mater.* **2011**, *23*, 1387.
(13) Switzer, J. R.; Ethier, A. L.; Flack, K. M.; Biddinger, E. J.; Gelbaum, L.; Pollet, P.; Eckert, C. A.; Liotta, C. L. *Ind. Eng. Chem. Res.* **2013**, *52*, 13159.
(14) Mafra, L.; Čendak, T.; Schneider, S.; Wiper, P. V.; Pires, J.; Gomes, J. R. B.; Pinto, M. L. *J. Am. Chem. Soc.* **2017**, *139*, 389.
(15) Inagaki, F.; Matsumoto, C.; Iwata, T.; Mukai, C. *J. Am. Chem. Soc.* **2017**, *139*, 4639.
(16) Lun, D. J.; Waterhouse, G. I. N.; Telfer, S. G. *J. Am. Chem. Soc.* **2011**, *133*, 5806.
(17) Li, D.; Furukawa, H.; Deng, H.; Liu, C.; Yaghi, O. M.; Eisenberg, D. S. *Proc. Natl. Acad. Sci. U. S. A.* **2014**, *111*, 191.
(18) Chen, C.; Shimon, D.; Lee, J. J.; Didas, S. A.; Mehta, A. K.; Sievers, C.; Jones, C. W.; Hayes, S. E. *Environ. Sci. Technol.* **2017**, *51*, 6553.

Supporting Information

The Chemistry of CO_2 Capture in an Amine-Functionalized Metal-Organic Framework under Dry and Humid Conditions

Robinson W. Flaig,[†] Thomas M. Osborn Popp,[†, §] Alejandro M. Fracaroli,[†,‡] Eugene A. Kapustin,[†] Markus J. Kalmutzki,[†] Rashid M. Altamimi,[§] Farhad Fathieh,[†] Jeffrey A. Reimer,[§,#] and Omar M. Yaghi*[,†,§,#]

[†]Department of Chemistry, University of California-Berkeley: Kavli Energy NanoSciences Institute at Berkeley; and Berkeley Global Science Institute, Berkeley, California 94720, United States
[§]Department of Chemical and Biomolecular Engineering, University of California-Berkeley, Berkeley, California 94720, United States
[‡]Instituto de Investigaciones en Fisicoquímica de Córdoba, INFIQC−CONICET, Facultad de Ciencias Químicas, Departamento de Química Orgánica, Universidad Nacional de Córdoba, Ciudad Universitaria, X5000HUA Córdoba, Argentina
[§]King Abdulaziz City for Science and Technology (KACST), Riyadh 11442, Saudi Arabia
[#]Materials Sciences Division, Lawrence Berkeley National Laboratory;

Table of Contents

Section S1: General Methods

Chemicals used in this work:

Anhydrous *N,N*-dimethylformamide (DMF), and methanol were obtained from EMD Millipore Chemicals. Sodium azide, triphenylphosphine, anhydrous tetrahydrofuran (THF), di-*tert*-butyl dicarbonate (Boc_2O), magnesium nitrate hexahydrate, and 1,4-dioxane were purchased from Aldrich. Diethyl ether, cesium fluoride, [1,1′-Bis(diphenylphosphino)ferrocene]dichloropalladium(II), sodium hydroxide, and 1,4-dioxane were purchased from Fischer Scientific. 1,4-Dibromo-2,5-bis(bromomethyl)benzene was purchased from Spectrum Chemical Manufacturing Group. Other common solvents and reagents (e.g. ethanol, ethanolamine, magnesium sulfate) were obtained from other commercial sources and all chemicals in this work were used without further purification. 3-hydroxy-4-(methoxycarbonyl) phenylboronic acid pinacol ester was synthesized according to published methods.[1]

Analytical Techniques:

^{1}H and ^{13}C{^{1}H} NMR spectra were acquired on Bruker AVB-400 (400 MHz), and AV-300 (300 MHz) spectrometers at 297–300 K. Chemical shifts were calculated using the solvent resonances as internal standards (^{1}H: 7.26 ppm for $CHCl_3$, 2.50 ppm for DMSO; ^{13}C{^{1}H}: 77.00 ppm for $CDCl_3$, 39.51 ppm for DMSO-d_6). FT-IR spectra were collected in-house using a Bruker ALPHA Platinum ATR-FT-IR Spectrometer equipped with a single reflection diamond ATR module. High Resolution Electrospray Ionization mass (HR-ESI) was acquired on an Finnigan LTQ FT (Thermo Electron Corporation) instrument, using either negative or positive modes and by direct injection of methanol solutions of the samples using syringe pump with a flow rate of 5 μL min^{-1}. Column chromatography was performed on silica gel purchased from Sorbent Technologies (standard grade, 60 Å, 40–63 μm). Analytical thin layer chromatography (TLC) was performed on Whatman 250 μm-thick silica gel 60 plates with a fluorescent indicator. Visualization of TLC spots was accomplished under UV light (λ = 254 nm). Powder X-ray diffraction data were collected using a Bruker D8-advance θ-θ diffractometer in parallel beam geometry employing Cu Kα1 line focused radiation at 1600 W (40 kV, 40 mA) power and equipped with a position sensitive detector with at 6.0 mm radiation entrance slit. Samples were mounted on zero background sample holders by dropping powders from a wide-blade spatula and then leveling the sample with a razor blade. Data were collected using a 0.01˚ 2θ step scan from 1 – 45˚ with exposure time of 3 s per step.

Section S2: Synthesis of Organic Linker

General synthetic scheme for linker synthesis:

The synthesis of 3-hydroxy-4-(methoxycarbonyl)phenylboronic acid pinacol ester (**1**), was carried out according to the reported procedure[1], on a multigram scale. Organic linker **4** was prepared by a two-fold Suzuki coupling of **1** and the dibromide **2** to give the corresponding dimethyl terphenyldicarboxylate derivative **3**. The dicarboxylic acid linker **4** was obtained by saponification of the methyl ester **3**. The general procedure is summarized in Scheme S1.
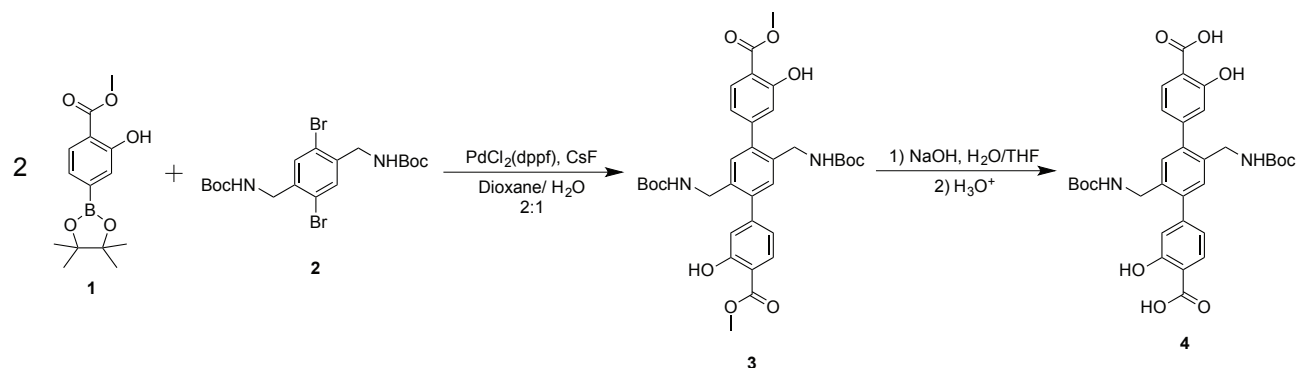
Scheme S1. General synthetic scheme for synthesis of organic linker 4.

Synthesis of 2,5-dibromo-1,3-di-*^{t}*butyl-benzylcarbamate (2)
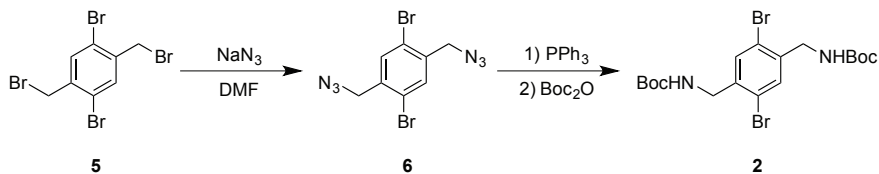
**Scheme S2.** Synthetic pathway for 2,5-dibromo-1,3-di-*^{t}*butyl-benzylcarbamate (2).

Commercially available 1,4-Dibromo-2,5-bis(bromomethyl)benzene (**5**, 1.6 g, 3.93 mmol), and sodium azide (1.0 g, 15.5 mmol) were added to a 250 mL three necked round bottom flask. The flask was evacuated and the atmosphere was replaced with dry nitrogen. This process was repeated three times to generate an air-free atmosphere in the reaction vessel. Anhydrous *N,N*-dimethylfomamide (50 mL) was then added to the flask under nitrogen and the solution was heated to 65 °C and stirred for 14 h. The reaction mixture was cooled to room temperature and then poured into a 250 mL separatory funnel. Diethyl ether (50 mL) was added to funnel and the mixture was then extracted with deionized water (3 · 50 mL) and brine (20 mL). The organic phase was dried over anhydrous magnesium sulfate, filtered, and evaporated to approximately 5 mL. THF (50 mL) was added to the concentrate and the resultant solution was evaporated until approximately 5 mL of solvent remained. This process was repeated two more times to give a light-yellow THF concentrate that was transferred to a three neck round bottom flask (RBF) for the next reaction without further purification [the product of the azidation reaction (**6**) was not isolated due to its potentially explosive nature].

THF (50 mL) was added to the RBF containing **6**, and the solution was degassed by bubbling with dry nitrogen for 30 minutes. Triphenylphosphine (2.3 g, 8.65 mmol) was added to the solution under nitrogen, and the reaction mixture was heated 60 °C and stirred for 2 h. Deionized water (4 mL) was then

added and the reaction mixture was left to stir at the same temperature for 14 additional hours. The reaction mixture was cooled to room temperature and di-*tert*-butyl dicarbonate [(Boc)$_2$O, 2.0 mL, 8.66 mmol] was added under nitrogen. This mixture was stirred at room temperature for 8 h, and ethanolamine (0.3 mL, 4.97 mmol) was added. The reaction mixture was left to stir under nitrogen at room temperature for another 3 h before the THF was evaporated. The yellow oil obtained was then transferred to a 250 mL separatory funnel and ethyl acetate (75 mL) was added. The mixture was extracted with deionized water (3 x 20 mL) and brine (20 mL), dried over anhydrous magnesium sulfate and evaporated to give a solid that was then purified by column chromatography (CH$_2$Cl$_2$:AcOEt 25:1). The product 2,5-dibromo-1,3-di-^{t}butyl-benzylcarbamate (**2a**) was obtained as a white powder in 70% yield (2.39 g). ^{1}H NMR (600 MHz, CDCl$_3$) δ [ppm]: 7.51 (s, 2H), 5.07 (t, J = 6.3 Hz, 2H), 4.31 (d, J = 6.4 Hz, 4H), 1.45 (s, 18H). ^{13}C NMR (151 MHz, CDCl$_3$) δ [ppm]: 155.81, 138.97, 133.24, 122.38, 80.11, 44.35, 28.50. ESI-HRMS calculated for C$_{18}$H$_{26}$Br$_2$N$_2$O$_4$Na$^+$: 515.0157, Found: 515.0153.

Synthesis of 2,5- Dimethyl 2',5'-bis(((tert-butoxycarbonyl)amino)methyl)-3,3''-dihydroxy-[1,1':4',1''-terphenyl]-4,4''-dicarboxylate (diamino linker ester, 3)
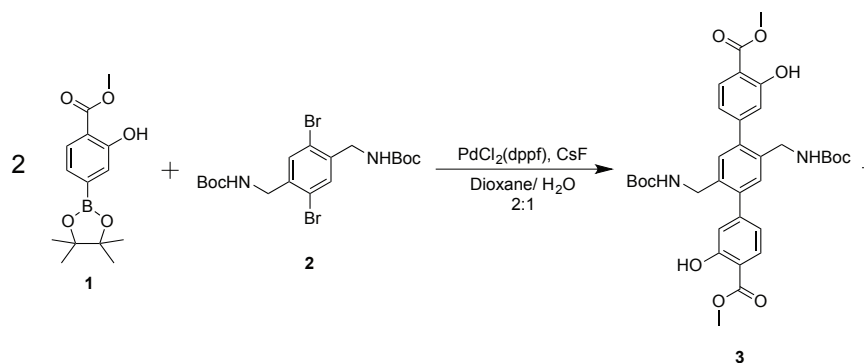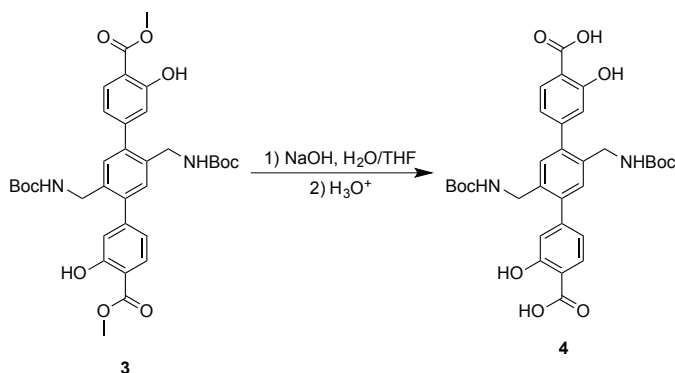

Scheme S3. Synthetic path for Dimethyl 2',5'-bis(((tert-butoxycarbonyl)amino)methyl)-3,3"-dihydroxy-[1,1':4',1''-terphenyl]-4,4"-dicarboxylate (**3**).

The synthesis of dimethyl 2',5'-bis(((tert-butoxycarbonyl)amino)methyl)-3,3''-dihydroxy-[1,1':4',1''-terphenyl]-4,4''-dicarboxylate (**3**) was accomplished via the two-fold Suzuki coupling outlined in scheme S1. A clean, oven dried, 3 neck round bottom flask attached to a Schlenk line apparatus with equipped reflux condenser was charged with 1.42 g (5.10 mmol) 3-hydroxy-4-(methoxycarbonyl) phenylboronic acid pinacol ester (**1**) and 2.77 g (18.2 mmol, 3.57 eq) of cesium fluoride. The flask and its contents were then evacuated and refilled with inert house nitrogen atmosphere. This process was repeated three times to ensure an anhydrous and oxygen-free reaction environment. In a separate flask, 14.6 mL of anhydrous 1,4-dioxane and 7.30 mL of deionized water were combined and then bubbled with dried house N$_2$ for 30 min. to deoxygenate the resulting mixture. 1.200 g (2.43 mmol) of di-*tert*-butyl ((2,5-dibromo-1,4-phenylene)bis(methylene))dicarbamate (**2**) were dissolved in the resultant solvent mixture under N$_2$ pressure and the solution was then added to the three neck round bottom flask containing the 3-hydroxy-4-(methoxycarbonyl) phenylboronic acid pinacol ester and cesium fluoride under N$_2$ pressure along with 0.0889 g (0.121 mmol, 0.0237 eq) [1,1′-Bis(diphenylphosphino)ferrocene]dichloropalladium(II). The reaction mixture was heated to 90° C using an oil bath and refluxed for 24 h. The resulting two layer (top-dark opaque brown, bottom-transparent colorless) solution was tested for completion with thin layer chromatography (25:1 dichloromethane: ethyl acetate) which provided evidence of the presence of mono- and di-coupled products. The reaction mixture was poured into a 500 mL separatory funnel with ca. 80 mL of ethyl acetate. 20 mL of a saturated NH$_4$Cl solution were added to the mixture in the separatory funnel and the organic phase was collected. The aqueous phase was extracted with 20 mL of ethyl acetate

and the combined organic phases were dried over anhydrous magnesium sulfate, filtered and evaporated to a brown powder. This crude product was purified by column chromatography (CH_2Cl_2:AcOEt 25:1) and the purified product (**3**) was obtained in 46% yield (0.711 g). 1H NMR (600 MHz, DMSO-$d6$) δ 10.60 (s, 2H), 7.86 (d, J = 8.0 Hz, 2H), 7.39 (t, J = 6.0 Hz, 2H), 7.25 (s, 2H), 7.00 – 6.94 (m, 4H), 4.11 (d, J = 6.0 Hz, 4H), 1.34 (s, 18H). ^{13}C NMR (151 MHz, DMSO-d_6) δ 168.95, 159.70, 147.31, 138.60, 135.30, 129.92, 120.37, 117.69, 112.01, 77.85, 52.45, 40.86, 28.12. MS (HR-ESI), m/z calcd. for $C_{34}H_{40}N_2O_{10}[(M+Na)^+]$: 659.2581, found: 659.2576.

Synthesis of 2',5'-bis(((tert-butoxycarbonyl)amino)methyl)-3,3''-dihydroxy-[1,1':4',1''-terphenyl]-4,4''-dicarboxylic acid (4)

Scheme S4. Synthetic path for 2',5'-bis(((tert-butoxycarbonyl)amino)methyl)-3,3''-dihydroxy-[1,1':4',1''-terphenyl]-4,4''-dicarboxylic acid (**4**).

A single-neck round bottom flask was charged with 0.700 g (1.10 mmol) of dimethyl 2',5'-bis(((tert-butoxycarbonyl)amino)methyl)-3,3''-dihydroxy-[1,1':4',1''-terphenyl]-4,4''-dicarboxylate (**3**). 27.5 mL of anhydrous THF were added to the flask and the solution was sonicated and stirred until complete dissolution of the reactant. In a separate flask 0.440 g (11.0 mmol, 10.0 eq) of anhydrous NaOH pellets were added to 27.5 mL of deionized water and the solution was stirred until the pellets were completely dissolved. The basic solution was subsequently added to the solution of *dimethyl* 2',5'-bis(((tert-butoxycarbonyl)amino)methyl)-3,3''-dihydroxy-[1,1':4',1''-terphenyl]-4,4''-dicarboxylate in THF to achieve a final NaOH concentration of 0.200 M and a final substrate concentration of 0.0200 M. The flask containing base and reactant was then attached to a Schlenk line apparatus with a reflux condenser equipped and was heated with an oil bath at 50 °C for 22 h. The reaction mixture was then cooled to room temperature and absence of starting material was confirmed by thin layer chromatography (1:1:1 dichloromethane: ethyl acetate: hexanes solvent mixture). The reaction mixture was acidified to pH 7 by addition of 1.157 mL of a 2M HCl solution. During acidification, a white solid formed in the reaction flask. 0.502 g of solid product **4** was collected by vacuum filtration (75.0 % yield). ^{1}H NMR (600 MHz, DMSO-$d6$) δ [ppm]: 14.00 (s, 2H), 11.35 (s, 2H), 7.86 (d, J = 7.9 Hz, 2H), 7.39 (t, J = 6.0 Hz, 2H), 7.26 (s, 2H), 6.95 (s, 2H), 4.12 (d, J = 5.9 Hz, 4H), 1.34 (s, 18H). ^{13}C NMR (151 MHz, DMSO-d_6) δ [ppm]: 171.67, 160.85, 155.60, 147.39, 138.72, 135.30, 130.14, 128.47, 120.18, 117.40, 111.94, 77.85, 40.89, 28.14. ESI-HRMS calculated for $C_{32}H_{36}N_2O_{10}Na^+$: 631.2268, Found: 631.2266.

Section S3: Synthesis of metal-organic frameworks (MOFs)

General notes for MOF synthesis:

Functionalized IRMOF-74-III compounds were prepared according to the procedure reported in literature.[1] $Mg(NO_3)_2 \cdot 6H_2O$ (160 mg, 0.62 mmol) and the desired organic linker (0.188 mmol) were added to a 20-mL scintillation vial with 15 mL anhydrous DMF. The vial was sonicated for 10 minutes and 1.0 mL of ethanol was added to the homogeneous solution followed by 1.0 mL of deionized water. The vial was sonicated again for 10 minutes sealed. The vial containing the resultant clear solution was placed in an isothermal oven at 120 °C for 20 h. After cooling to room temperature, the supernatant solution was removed by syringe and the crystalline solid MOF compound was immersed in 10 mL of anhydrous DMF for 3 h. The liquid was then decanted and replaced with another 10 mL of anhydrous DMF. This process was repeated three times per day for 3 days after which time the procedure was repeated with methanol during 2 days to obtain the solid with washed interior. After this time, the –boc protecting groups were quantitatively removed from the compounds following the procedure detailed in section S3. In order to avoid measuring CO_2 uptakes of the materials with protonated forms of the amino functionalities on the organic linkers, the MOFs were suspended in a 20% triethylamine solution in methanol for 30 min prior to activation. The solution within the pores of the resulting solid was removed under dynamic vacuum initially at room temperature and then by heating at 120 °C for 8 h. The guest free samples were analyzed by PXRD and their surface area was determined by nitrogen adsorption experiments.

Synthesis of IRMOF-74-III-(CH$_2$NHBoc)$_2$

The synthesis was realized according to the general procedure above, yielding 81% of off-white crystals. PXRD was collected on activated sample (guest free). The high degree of correspondence between the sample pattern and that of the simulated model indicates that the bulk material has the same crystal structure as the predicted by simulation (section S8). To determine the presence of functional groups in the MOF pores, we have performed ^{1}H NMR of digested samples in 50 mM DCl in a DMSO-d_6/D$_2$O mixture (section S7). The resonance peaks at 1.35 ppm (d, 9H) and 4.14 ppm (s, 2H) corresponding to the Boc protecting group and benzyl amine (-CH$_2$-) respectively; confirm the presence of -CH$_2$NHBoc functional group in the framework. IR (ATR), $\bar{v}_{max}$ [cm^{-1}]: 3360 (br w), 2977 (w), 1682 (s), 1580 (s), 1505 (m), 1431 (s) 1367 (s), 1249 (br s), 1219 (m) 1157 (s), 1025 (s), 940 (m), 890 (m), 847 (m), 790 (m), 722 (m), 696 (m) 602 (m).

Section S4: Thermal post-synthetic -Boc deprotection

General notes for thermal post-synthetic –Boc deprotection

The functionalized IRMOF-74-III crystals were subjected to solvent washing procedure described in section 3. The compounds were transferred using a glass pipette into a 10 mL reaction tube containing 3 mL of 2-ethyl-1-hexanol, 150 μL of ethylene glycol and 150 μL of deionized water. The heterogeneous mixture was subjected to 230 °C microwave heating for 10 minutes. The mixture was allowed to cool down to room temperature and the DMF and methanol solvent washing procedure was repeated. The obtained microcrystalline samples were analyzed by PXRD and ^{1}H NMR after digestion.

Thermal post-synthetic –Boc deprotection of IRMOF-74-III-(CH$_2$NHBoc)$_2$

The Boc protecting group was removed by microwave heating as described above. The yellow crystals of IRMOF-74-III-(CH$_2$NH$_2$)$_2$ were recovered in 98% reaction yield. PXRD was collected on activated sample (guest free). The high degree of correspondence between the sample pattern and that of the sample before the deprotection procedure indicates that the bulk material remains crystalline and with the same underlying topology after the post-synthetic deprotection (section S8). The successful Boc-deprotection was confirmed by the absence of the -Boc resonance peak at 1.31 ppm in the ^{1}H NMR of digested samples (section S7) in 50 mM DCl in a DMSO-d_6/D$_2$O mixture (Figure S8, Section 4). IR (ATR), $\bar{\nu}_{max}$ [cm^{-1}]: IR (ATR), $\bar{\nu}_{max}$ [cm^{-1}]: 3360 (br w), 2977 (w), 1682 (br w), 1580 (s), 1431 (s) 1367 (s), 1249 (br s), 1219 (m), 1198 (m),1157 (w), 1025 (s), 940 (m), 890 (m), 847 (m), 790 (m), 722 (m), 696 (m) 602 (m).

Section S5: Solid State NMR experiments

^{13}C and ^{15}N CP-MAS NMR experimental parameters

Solid state NMR spectra were collected using a 7.05 T magnet with a Tecmag Apollo spectrometer operating at 300.27 MHz for ^{1}H, 75.51 MHz for ^{13}C, and 30.43 MHz for ^{15}N. ^{13}C chemical shifts were externally referenced to the downfield resonance of adamantane at 38.48 ppm, and ^{15}N chemical shifts were externally referenced to glycine at 33.4 ppm. Experiments were performed using either a Doty 4-mm or Doty 5-mm triple resonance MAS probe operating in triple resonance ^{1}H/^{13}C/^{15}N mode. Magic angle spinning (MAS) was used to collect high-resolution NMR spectra at a spinning rate of 8 kHz. The magic angle was calibrated by maximizing the number and intensity of rotational echoes for the ^{79}Br resonance for KBr under MAS. ^{13}C and ^{15}N cross polarization (CP) experiments under the Hartmann-Hahn matching condition were performed with a ^{1}H 90° pulse time of 3.0 μs, and a contact time of 2 ms, using 80 kHz continuous-wave ^{1}H decoupling during signal acquisition. Spectra were collected with 2048 scans and a recycle delay time of 4 s, and were processed without apodization except where specified.

CO_2 gas loading and NMR sample preparation

All samples were packed into Doty 4 mm or 5 mm zirconia rotors in an argon atmosphere glovebox. The packed, uncapped rotor was then quickly transferred to a home-built gas dosing apparatus and vacuum was applied for 2 hours. After this period, the sample was exposed to 675 torr (900 mbar) $^{13}CO_2$ gas (Sigma-Aldrich, 99% atom ^{13}C) for 24 hours at room temperature. The pressure was monitored using an MKS Baratron capacitance manometer with a working range of 1-5000 torr. After exposure, the rotor was quickly capped and transferred to the magnet for NMR analysis to minimize any loss of CO_2. Significant CO_2 leakage, and correspondingly, changes to the ^{13}C and ^{15}N spectra (namely a loss of intensity from the carbamic acid resonance), was observed after several hours (12-24 hours) of MAS NMR data acquisition. However, this loss was minimized by keeping the length of each NMR experiment to around 2 hours. Water-exposed MOF samples were prepared following the procedure detailed in section S15. The water-exposed MOFs were then transferred to the gas dosing apparatus and exposed to $^{13}CO_2$ as described previously. The lab atmosphere was measured to be roughly 50 % RH using a chilled mirror setup described in section S15. A packed rotor was left uncapped and exposed to the lab atmosphere for 24 hours before loading with $^{13}CO_2$ as described. These ^{13}C and ^{15}N CP-MAS spectra are shown in figures S2 and S3 respectively.
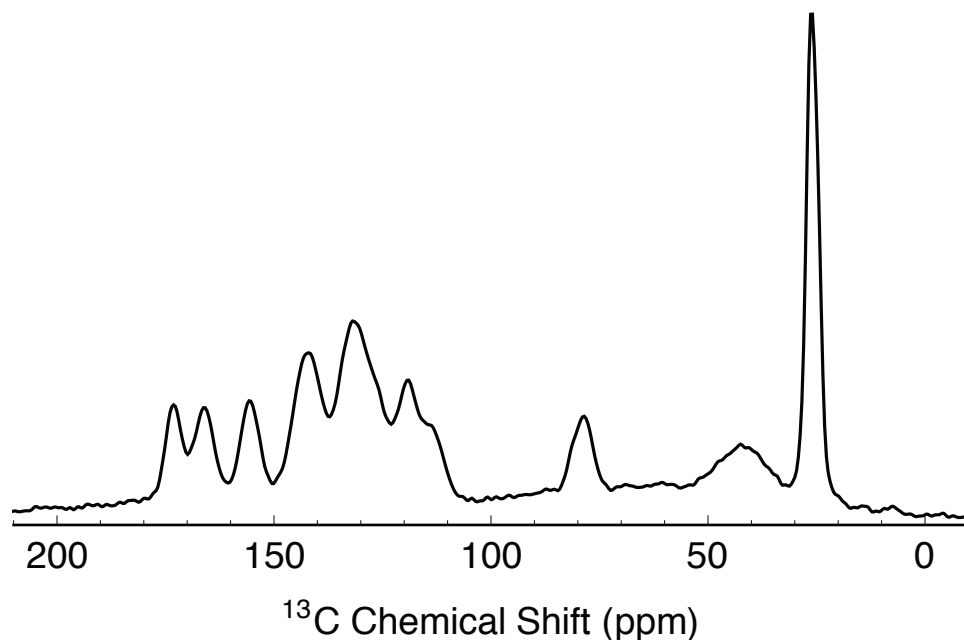
Figure S1. ^{13}C CP-MAS NMR of activated IRMOF-74-III-$(CH_2NHBoc)_2$ processed with 25 Hz line broadening. Note the significant peaks at approximately 155, 80, 40 and 25 ppm corresponding to the -Boc group, which are not present in the ^{13}C spectrum of the deprotected material.
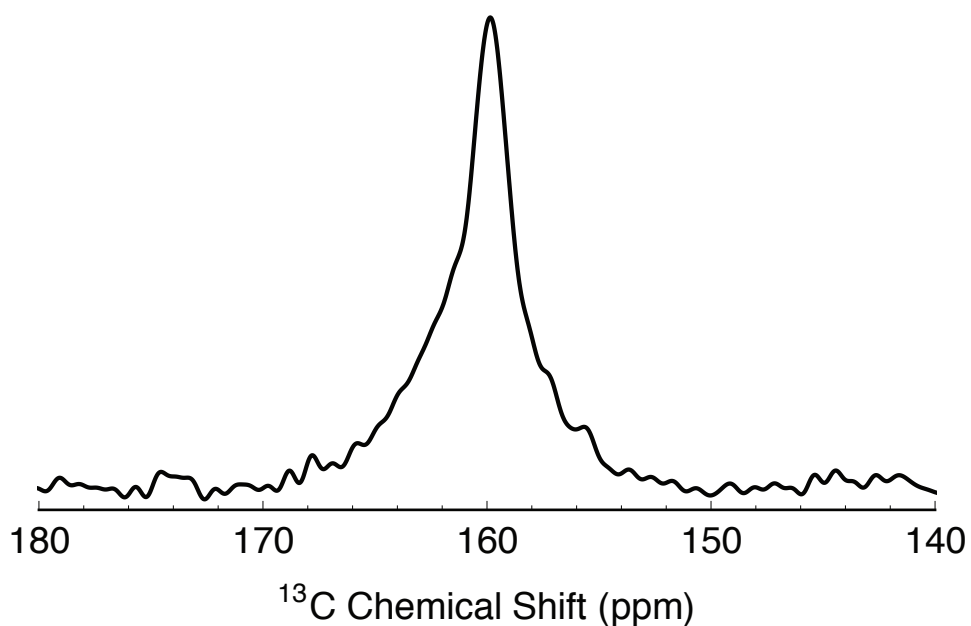
Figure S2. ^{13}C CP-MAS NMR of atmosphere-exposed (50% RH) IRMOF-74-III-$(CH_2NH_2)_2$ subsequently exposed to 675 mbar $^{13}CO_2$. Note the large peak with maximum at 160.3 ppm, however there is a loss of the right shoulder intensity between 160 and 155 ppm when compared

to the dry spectrum (main text figure 2b, red) and an increase in intensity for the left shoulder spanning through 164 ppm attributable to the increase in carbamate,
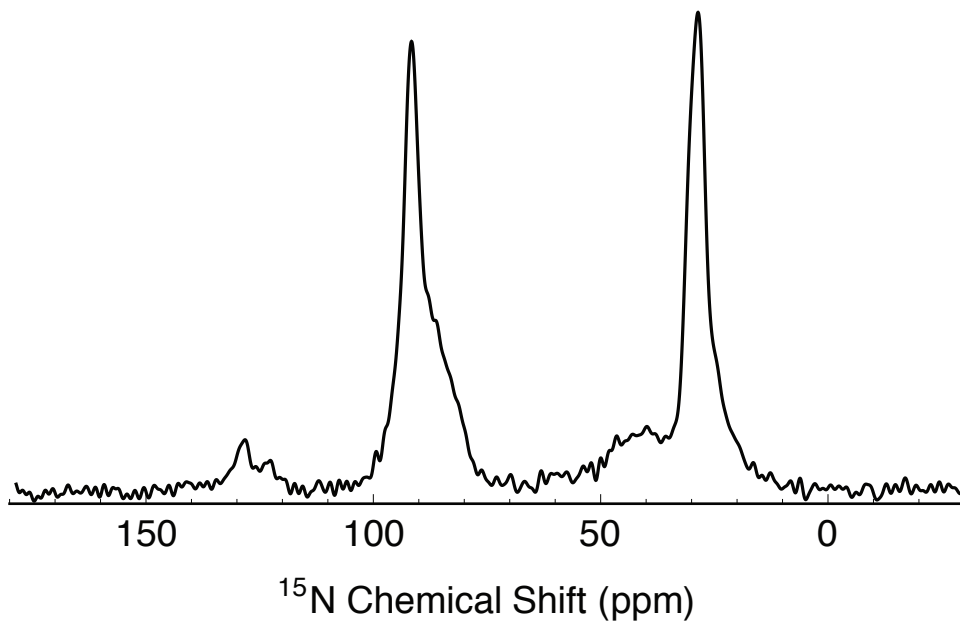
Figure S3. ^{15}N CP-MAS NMR of atmosphere-exposed (50% RH) IRMOF-74-III-$(CH_2NH_2)_2$ subsequently exposed to 675 mbar $^{13}CO_2$. The amine peak at 30 ppm has lost the splitting observed in the ^{15}N spectrum of the dry material. The broadening of the base of the resonance with a maximum at 91 ppm suggests that there is an increase in carbamate is formed in addition to carbamic acid, as well as a broad feature at around 40 ppm attributable to a small amount of ammonium.

Section S6: FT-IR spectra of activated MOFs

Cleavage of the –Boc protecting groups was confirmed by the disappearance of the stretching frequencies at 1682 ($v_{c=o}$) and 1157 (v_{c-o}) cm^{-1}. After exposure to dry CO_2 the appearance of an absorption band at 1692 cm^{-1} in IRMOF-74-III-$(CH_2NH_2)_2$ indicated carbamic acid ($v_{c=o}$) formation, consistent with stretching frequencies previously reported.[2] Further analysis of the FT-IR spectra revealed the absence of absorption bands typically assigned to carbamate moieties (1575 cm^{-1} [$v_{c=o}$]) after dry CO_2 loading.[2]
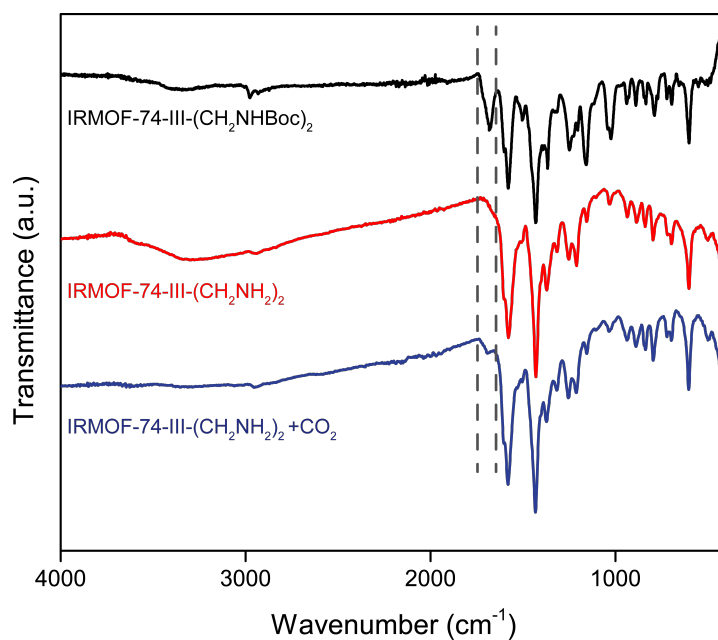
Figure S4. FT-IR (ATR) spectra of activated IRMOF-74-III-$(CH_2NHBoc)_2$ (black curve) and IRMOF-74-III-$(CH_2NH_2)_2$ (red curve) showing –Boc group cleavage as evidenced by the disappearance of peaks at and 1682 and 1157 cm^{-1}. After exposure to dry CO_2 (blue curve) we observe carbamic acid formation as evidenced by the appearance of a small peak at and 1694 cm^{-1}.

Section S7: Solution ^{1}H NMR of digested samples

General procedure

Typically, for the digestion of the MOF samples ca. 10 mg of functionalized IRMOF-74-III were dried in air ca. 12 h after solvent washing with DMF. Then 0.5 mL of DMSO-d_6 and 10 µL of DCl in D_2O (35 wt. %), were added. The suspension was sonicated 1 min and left at room temperature until the solution clarified. The ^{1}H NMR spectra were recorded after 10 min.

Spectroscopic results
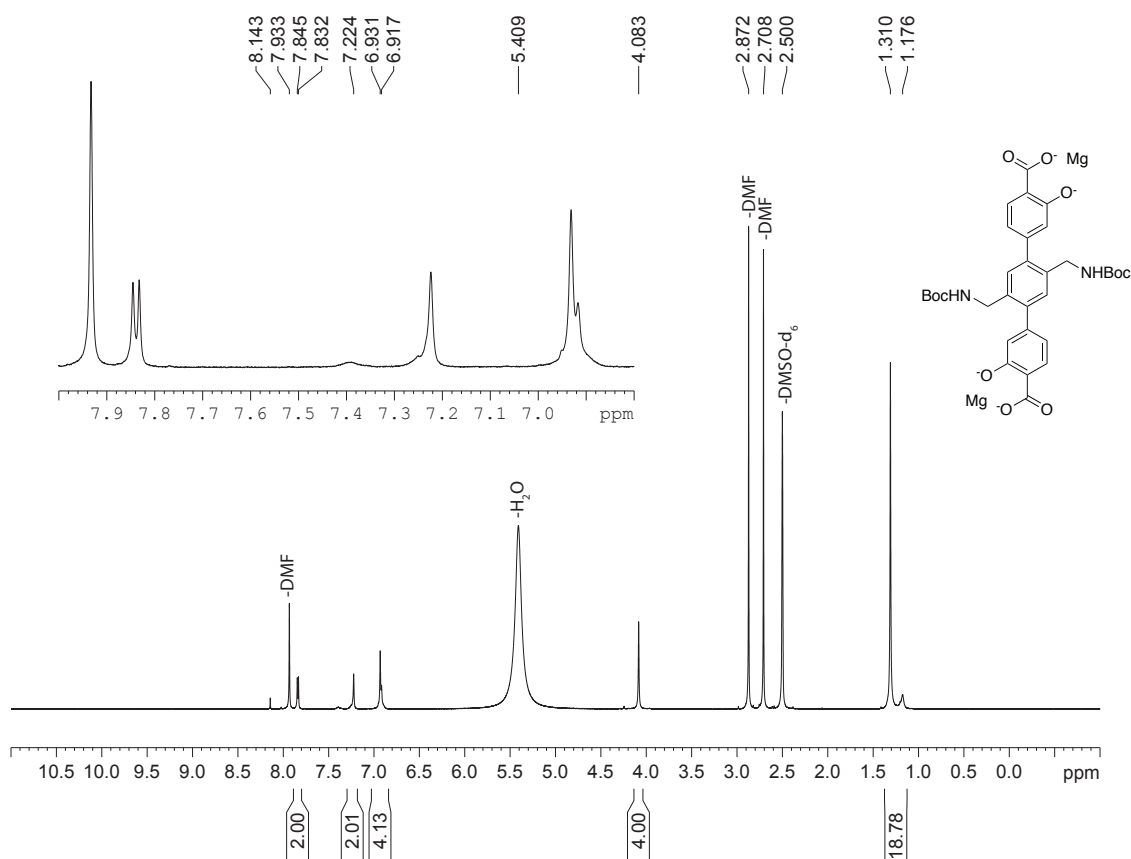
Figure S5. ^{1}H NMR spectra of IRMOF-74-III-(CH$_2$NHBoc)$_2$ digested sample in 50 mM DCl/DMSO-d6/D_2O mixture. Inset, expanded aromatic region in the spectra.
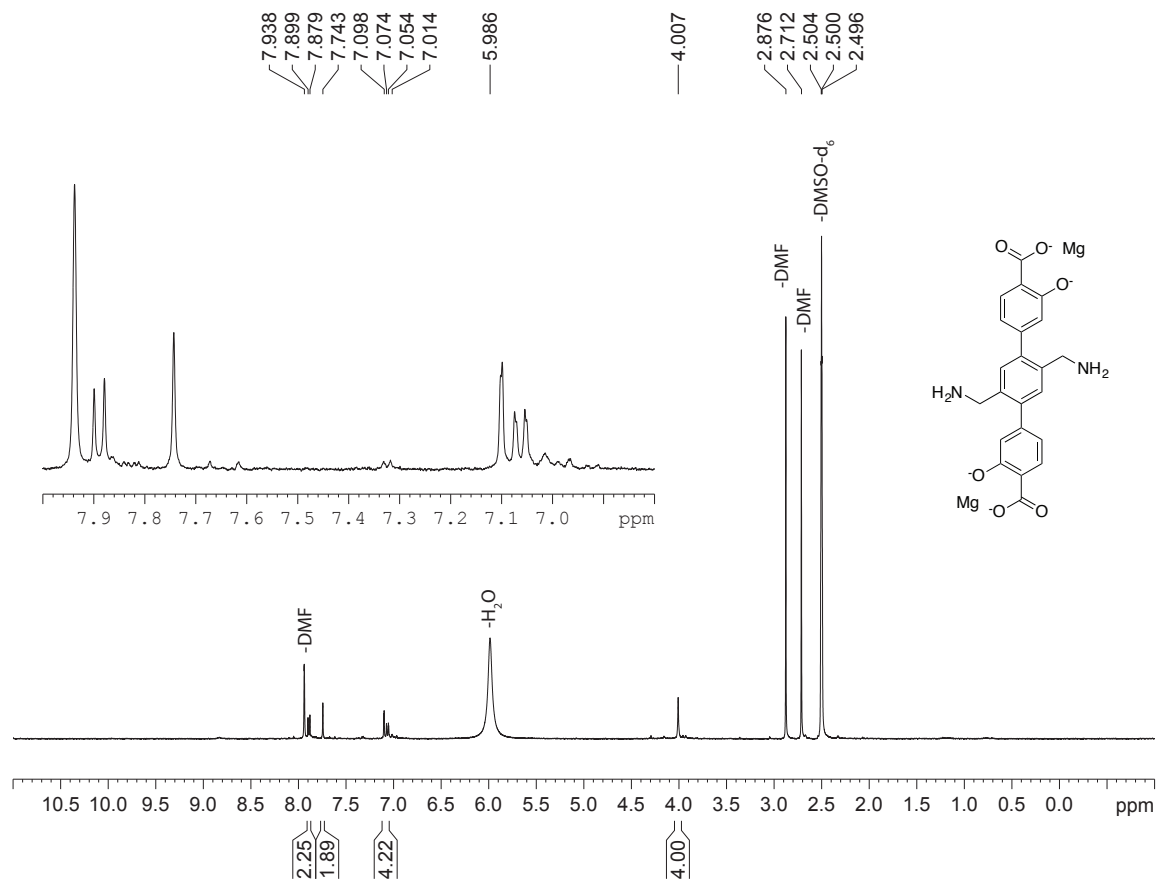
Figure S6. ^{1}H NMR spectra of IRMOF-74-III-$(CH_2NH_2)_2$ digested sample in 50 mM DCl/DMSO-d6/D_2O mixture. Inset, expanded aromatic region in the spectra.

Section S8: Powder X-ray diffraction (PXRD) characterization
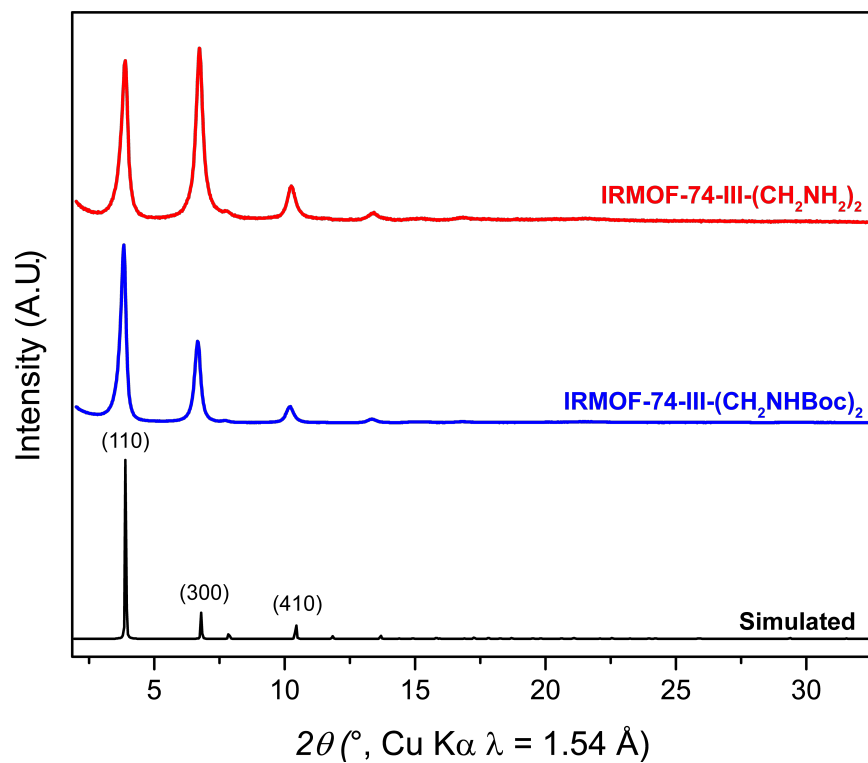
Figure S7. PXRD pattern of simulated IRMOF-74-III (black), activated IRMOF-74-III-(CH$_2$NHBoc)$_2$ (blue), and IRMOF-74-III-(CH$_2$NH$_2$)$_2$ (red).

Section S9: Nitrogen adsorption measurements

All nitrogen isotherms were measured using a Quantachrome Qudrasorb EVO instrument. Ca. 70 mg of guest free samples in 9 mm bulb gas cells were charged with argon to avoid air contamination and the cells were mounted on the instrument. A liquid nitrogen bath was used to maintain a temperature of 77 K for each measurement. Ultra-high-purity grade N_2 (Praxair, 99.999% purity) was used throughout the adsorption experiments. 46 adsorption and 16 desorption points were collected. The BET surface areas were estimated according to established procedures. Slight discrepancies in surface area measurements are likely caused by the same phenomena detailed in our study of IRMOF-74-III-(CH_2NH_2)[1], which detail the presence of a H4 type hysteresis loop[3] attributed to intercrystalline voids in the sample.[4]
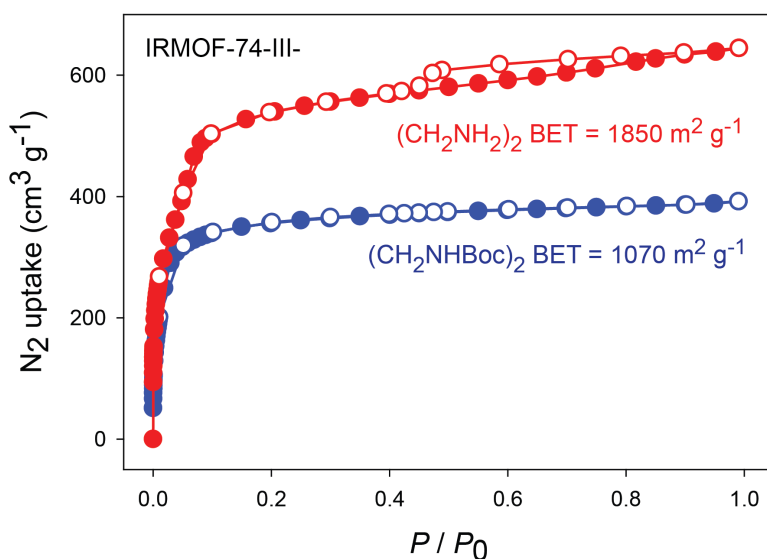
Figure S8. Nitrogen adsorption isotherms for IRMOF-74-III-$(CH_2NHBoc)_2$ (blue), and IRMOF-74-III-$(CH_2NH_2)_2$ (red) at 77 K. The inset text details the experimental BET surface areas for the two compounds.

Section S10: Details of CO_2 adsorption measurements

All CO_2 isotherms were measured immediately after activation procedures detailed above unless otherwise described. Measurements were performed using a Quantachrome Autosorb instrument. Ca. 70 mg of guest free samples in 9 mm bulb gas cells were charged with argon to avoid air contamination and the cells were mounted on the instrument. A water bath was used to maintain a temperature of 298 K for each measurement. CO_2 (Praxair, 99.998% purity) was used throughout the adsorption experiments. 55 adsorption and 12 desorption points were collected.
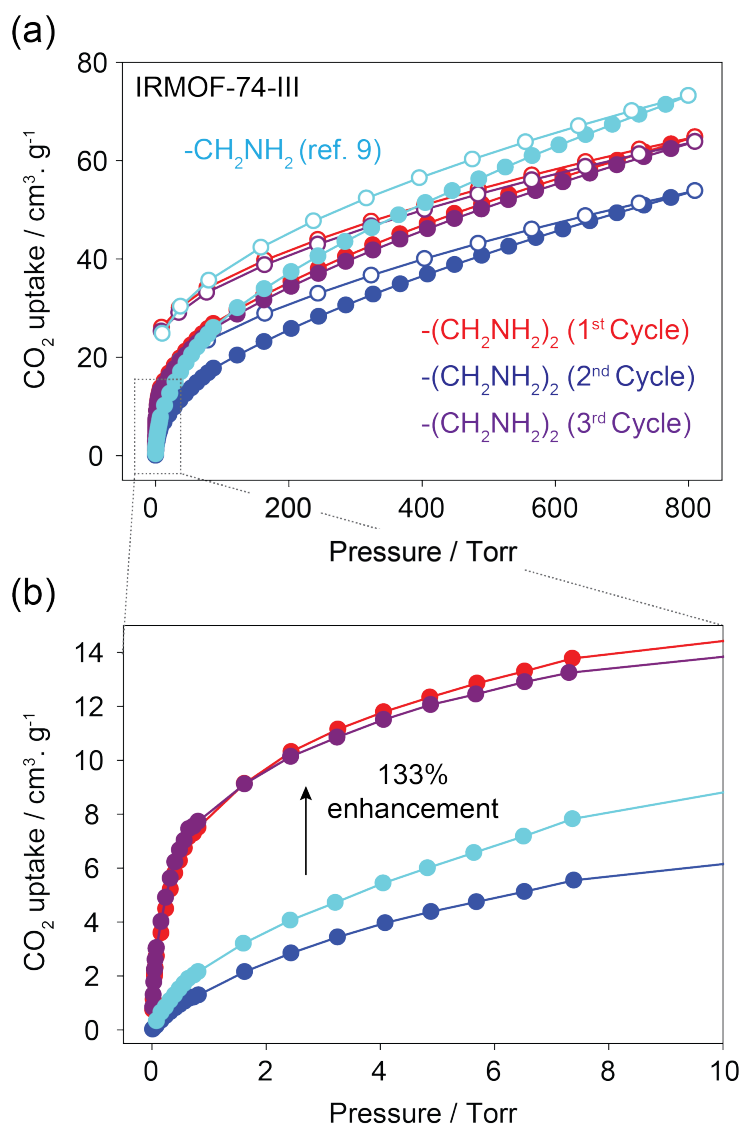
Figure S9. (a) Carbon dioxide isotherms for IRMOF-74-III-$(CH_2NH_2)_2$ and IRMOF-74-III-CH_2NH_2 at 25 °C. In red, after activation (first cycle); in blue, after first carbon dioxide isotherm (second cycle); and in purple, after 120 °C heating 2 h (third cycle) in cyan, carbon dioxide isotherm for IRMOF-74-III-CH_2NH_2 for comparison. (b) expansion of the low pressure range.

Section S11: Modeling of IRMOF-74-III-(CH$_2$NH$_2$)$_2$ and resultant distances

To model the inter-methylene distances in question in IRMOF-74-III-(CH$_2$NH$_2$)$_2$, we began with a crystal structure of Mg-MOF-74 previously published to establish O-Mg bond distances and inter-linker spacing for the material.[5] We then constructed, from scratch, a model of Mg-IRMOF-74-III in BIOVIA Materials Studio 8.0 using these distances as heuristics for the structure. The structure was optimized using the *Forcite* module in the software. From there, we modeled the amines in a staggered orientation (as logically follows from the argument with respect to steric hindrance in the main text) and re-optimized the structure. Finally, calculated PXRD patterns were generated using the *Reflex* module in the software. These patterns were used for comparisons in section S8.

Section S12: Thermogravimetric analysis

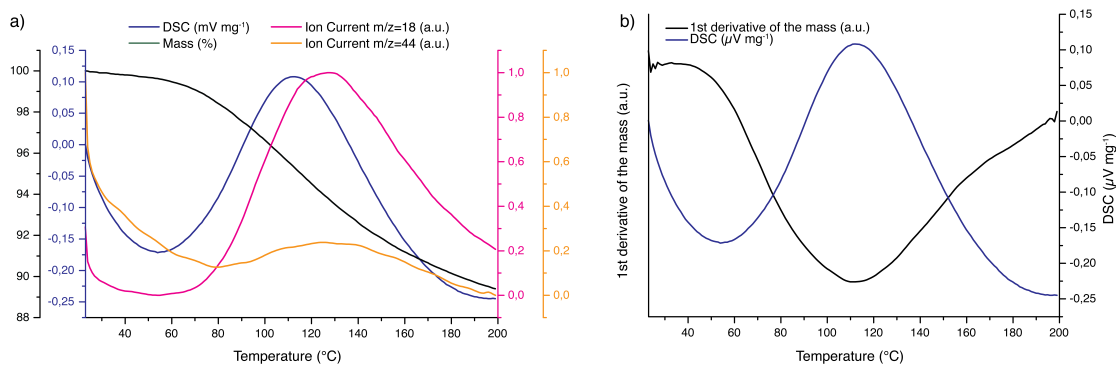**Dry IRMOF-74-III-(CH₂NH₂)₂ sample**

Coupled DSC-TGA studies were performed under a flow of CO_2 (20 ml min^{-1}) in a Netzsch Jupiter, STA 449 F5 apparatus. MS spectra were recorded on a Netzsch Aëolos QMS 403D. IRMOF-74-III-(CH₂NH₂)₂ was loaded with CO_2 (see above) prior to DSC-TGA analysis. About 7 mg of sample were filled into an aluminum sample holder. The samples were subjected to a heating rate of 10 °C min^{-1} and a maximum temperature of 200 °C under a CO_2 (20 ml min^{-1}) atmosphere. A mass loss corresponding to 12 % is observed (Fig. S10), however an onset temperature for this mass loss could not be determined. The first derivative of the TGA curve coincides with the maximum of an endothermic effect in the DSC curve which is correlated to the loss of CO_2. The porous nature of IRMOF-74-III-(CH₂NH₂)₂ does not allow for the determination of a bond energy, due to ineffectual heating of the mostly voided activated sample. The thermal energy at 47 °C (center of the first derivative of the mass loss) correlates to approximately 89.6 kJ, which is in good agreement with calculated values for the activation energy of bond cleavage in carbamic acid.[6]

Humidified IRMOF-74-III-(CH₂NH₂)₂ sample

20 mg of IRMOF-74-III-(CH₂NH₂)₂ was transferred into an aluminum sample holder, after humidification following the procedure and subsequently exposed to CO_2 (flow-rate 40 ml min^{-1}) inside the STA 449 F5 for 24 hours. After CO_2 loading the sample was subjected to a heating rate of 10 °C min^{-1} and a maximum temperature of 200 °C under a CO_2 atmosphere. The measurement shows a mass loss corresponding to 10 % with an onset at 65 °C (Fig. S11). The mass loss is attributed to both H_2O and CO_2 as evidenced by simultaneously recorded MS spectra. The first derivative of the TGA curve coincides with the maximum of an endothermic effect in the DSC curve which is correlated to the loss of CO_2 and the desorption of H_2O. The MS signals for CO_2 and H_2O both occur at the same temperature as the endothermic DSC peak. The fact that CO_2 is liberated at significantly higher temperatures (peak centered around 130 °C) indicates the presence of a different species (ammonium carbamate), which is in good agreement with the NMR measurements performed.
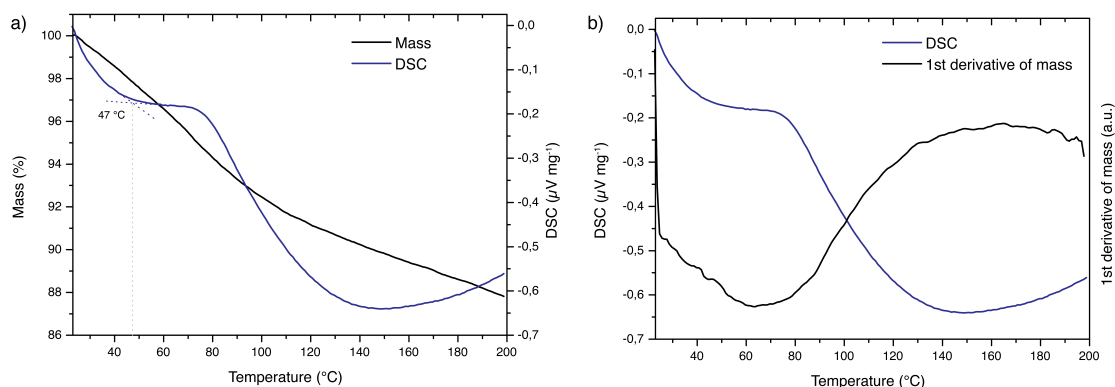
Figure S10. TGA-DSC measurement of a dry CO_2 loaded sample of IRMOF-74-III-(CH₂NH₂)₂. a) The blue line represents the DSC curve which shows an endothermic peak corresponding to the liberation of CO_2 centered around 80 °C. The onset at 47 °C correlates to the activation energy for the bond cleavage. b) The first derivative of the TG curve (black) shows one broad beak that correlates well with the endothermic peak in the DSC curve.

Figure S11. TGA-DSC-MS measurement of a humidified, CO_2 loaded sample of IRMOF-74-III-$(CH_2NH_2)_2$. a) The blue line represents the DSC curve which shows an endothermic peak corresponding to the liberation of CO_2 centered around 120 °C. The onset at 65 °C correlates to the activation energy for the bond cleavage (123 kJ). b) The first derivative of the TG curve (black) shows one broad beak that correlates well with the endothermic peak in the DSC curve.

# Section S13: Dynamic CO_2 capture in the presence of water

To compare the dynamic capacity of IRMOF-74-III-$(CH_2NH_2)_2$ to the previously reported -CH_2NH_2 compound, CO_2 breakthrough experiments were conducted using dry (0% RH) and wet (65% RH) streams of 16% (v/v) CO_2 in nitrogen. A stainless steel column (10 cm length × 0.6 cm diameter) was packed with 240 mg (0.53 mmol) of IRMOF-74-III-$(CH_2NH_2)_2$ to be used as an adsorbent bed. The mixed gas streams were introduced to the column and the effluent gasses were monitored by a mass spectrometer. Breakthrough time was determined when the effluent CO_2 concentration reached 5% of the influent concentration, similar to other studies. Under exposure to the dry gas stream, the IRMOF-74-III-$(CH_2NH_2)_2$ adsorbent bed held CO_2 for 900 ± 10 s g^{-1}, which is equivalent to a kinetic CO_2 adsorption capacity of 1.2 mmol g^{-1} (Figure S12). The breakthrough experiment was repeated two times, and between each trial, the adsorbent bed was flushed with dry nitrogen gas and heated to 120 ºC for 30 minutes to remove all CO_2 molecules chemisorbed to the surface. The kinetic adsorption capacity remained essentially unchanged when the material was exposed to the wet gas stream where the IRMOF-74-III-$(CH_2NH_2)_2$ adsorbent bed held CO_2 for 890 ± 10 s g^{-1}, which is equivalent to a kinetic CO_2 adsorption capacity of 1.2 mmol g^{-1}. These results constitute a 34% increase in the dynamic capacity of the IRMOF-74-III-$(CH_2NH_2)_2$ material over its monoamine functionalized counterpart. Interestingly, when comparing the breakthrough performance of the material exposed to a wet gas mixture to that of the material exposed to a dry gas mixture, the breakthrough times are nearly identical as previously mentioned. However, the material requires a significantly greater amount of time for the effluent gas to match the CO_2 composition of the influent gas when the gas mixture is humidified. This supports our hypothesis that the mechanism of CO_2 uptake is altered in the presence of water and the kinetic consequence of using two amines to capture one molecule of CO_2 causes slower overall uptake.
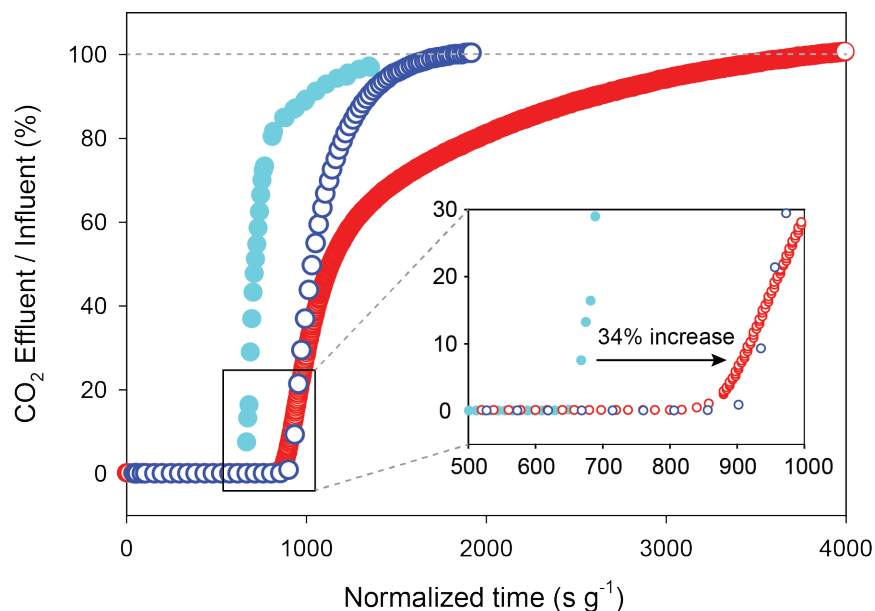
Figure S12. Breakthrough curves for IRMOF-74-III-$(CH_2NH_2)_2$ under dry conditions (dark blue empty markers) and wet conditions (red empty markers), and for comparison, IRMOF-74-III-CH_2NH_2 under wet conditions (cyan filled markers).

Section S14: Control experiment mitigating the impact of base pre-treatment

In order to fully neutralize the amine moieties in the MOF pores leaving them accessible to reaction with CO_2, the crystalline MOF powders were washed with a triethylamine in methanol solution as described in section S2. To ensure that treatment of IRMOF-74-III-$(CH_2NH_2)_2$ with triethylamine-methanol solution would only affect the primary amine moieties covalently bound to the organic struts of the material, we subjected an analogous compound, IRMOF-74-III-CH_3, to the same washing conditions. CO_2 uptake capacity was obtained by measuring isotherms at 298 K (25 °C, Figure S13) for IRMOF-74-III-CH_3 with and without base treatment. We observed no significant differences in the uptake behavior of the material regardless of whether or not triethylamine base was utilized in preparation of isotherm measurement, indicating that base treatment does not affect the underlying MOF structure, nor does it serve to alter the environment of the metal clusters present.
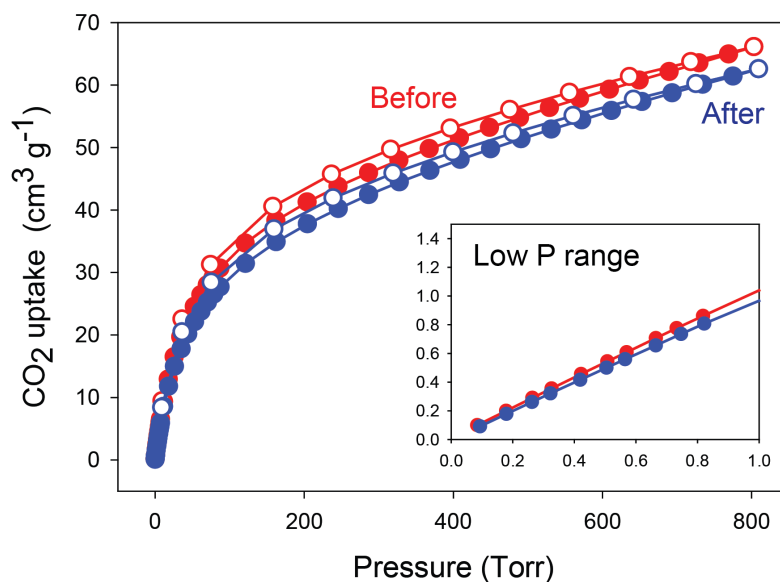
Figure S13. CO_2 isotherms for IRMOF-74-III-CH_3 at 25 °C. In red, before; in blue, after trimethylamine treatment. The inset shows that the low pressure uptake of carbon dioxide does not change upon treatment with triethylamine solution.

Section S15: Humidification of IRMOF-74-III-(CH$_2$NH$_2$)$_2$ samples

Samples of activated IRMOF-74-III-(CH$_2$NH$_2$)$_2$ were saturated with water vapor at a relative humidity (RH) values of RH = 95% by using a HygroCal100 Humidity Generator/Calibrator (Michell Inc, MA, USA) controlled humidity chamber. To generate uniform humidity across the chamber, the HygroCal 100 humidity generator is equipped with seven HygroSmart HS3 capacitive humidity sensors with ±0.8% accuracy. The bias error was eliminated by using an external standard reference precision dew-point meter (chilled mirror with ±0.2 °C$_{dew-point}$ accuracy). Ultimately, the humidity measurements were taken with the overall uncertainty of ±1%.

For each humidification, *ca*. 30 mg of activated MOF was transferred into the appropriate container (Al pan for TGA-DSC-MS, Rotor for CP-MAS-NMR) in a nitrogen-filled glove box and placed inside the sealed HygroCal100 humidity chamber in an uncapped 4 mL vial. To minimize atmospheric CO$_2$ interaction with the MOF during humidification, the chamber was purged with ultra-pure nitrogen (99.999%) and kept under 0-0.5% RH for at least 5 minutes. While nitrogen flowed through the humidity chamber, the vials were transferred to the chamber and after another 1-2 minutes the humidity value stabilized back to 0-0.5%. Then, the nitrogen flow was stopped and the water loading experiment commenced by increasing the relative humidity inside the chamber from 0-0.5% to 95% with transition period of less than 2 minutes. The samples were kept inside the humidity controlled chamber for 24 hours to ensure that the samples were saturated with water at the specified RH values.

Section S16: References

1. Fracaroli, A. M.; Furukawa, H.; Suzuki, M.; Dodd, M.; Okajima, S.; Gándara, F.; Reimer, J. A.; Yaghi, O. M. *J. Am. Chem. Soc.* **2014**, *136*, 8863-8866.
2. Masuda, K.; Ito, Y.; Horiguchi, M.; Fujita, H. *Tetrahedron* **2005**, *61*, 213-229
3. Doonan, C. J.; Morris, W.; Furukawa, H.; Yaghi O. M. *J. Am. Chem. Soc*. **2009**, *131*, 9492-9493.
4. Vishnyakov, A.; Ravikovitch, P. I.; Neimark, A. V.; Bülow, M.; Wang, Q. M. *Nano Lett*. **2003**, *3*, 713-718.
5. Dietzel, P. D. C.; Blom, R.; Fjellvåg, H. *Eur. J. Inorg. Chem.* **2008**, *2008*, 3624-3632.
6. Mora, J. R.; Tosta, M.; Domínguez, R. M.; Herize, A.; Barroso, J.; Córdova, T.; Chuchani, G. *J. Phys. Org. Chem.* **2007**, *20*, 1021-1031.